

# Mapping Gaseous Pollutant Using Quadcopter on Autonomous Waypoint Navigation

Muhammad Rivai<sup>a,1</sup>, Rudy Dikairono<sup>a,2</sup>, Irfan Fachrudin Priyanta<sup>a,3</sup>

<sup>a</sup>Department of Electrical Engineering, Institut Teknologi Sepuluh Nopember, Surabaya, 60111, Indonesia  
E-mail: <sup>1</sup>muhammad\_rivai@ee.its.ac.id; <sup>2</sup>rudydikairono@ee.its.ac.id; <sup>3</sup>irfan.fachrudin12@mhs.ee.its.ac.id

---

**Abstract**— Air pollution is a condition in which air quality is damaged and contaminated with substances that are harmful to living things. Along with the increase in the number of motorized vehicles and industrial areas in Indonesia can increase the level of air pollution. Generally, monitoring systems for air pollution are carried out using gas sensors at certain points. However, this method takes a lot of time and cost, as well as low spatial resolution for a wide area. The quadcopter is a type of Unmanned Aerial Vehicle that can move automatically according to the tracking system based on the waypoints of the Global Positioning System. In this study, a quadcopter equipped with a gas sensor is used to map air pollution levels. Mission Planner software is used to determine the waypoints of the quadcopter. The proportional-integral-derivative (PID) control is used to maintain the altitude of the quadcopter while hovering. The gas level can be stored and accessed online on the webserver, in which the results of the gas mapping are displayed on Google Earth. The experiment results show that the measurement of carbon monoxide using the semiconductor gas sensor has an error of 9.6%. The quadcopter can route all the provided waypoints for its navigation. The quadcopter can also maintain the height according to the offered altitude setpoints with a steady-state error of 21.4 % and 15.75%, respectively.

**Keywords**— air pollution; gas sensor; global positioning system; quadcopter; waypoints.

---

## I. INTRODUCTION

Air pollution, according to the Indonesian Government Regulation for the Control of Air Pollution, is the inclusion or exclusion of substances, energy, and other components into the ambient air by human activities, which results in air quality dropping to a certain level. Many large cities have ambient air pollution concentrations exceeding the standards allowed by the World Health Organization (WHO). Air pollution in cities is mostly contributed by the transportation sector [1]. Uncontrolled population growth and lack of mass transportation exacerbate this level of pollution. The rest is produced by the industrial sector [2] and household air pollutants [3]. The major air pollutants are carbon monoxide (CO), ozone (O<sub>3</sub>), nitrogen dioxide (NO<sub>2</sub>), and sulfur dioxide (SO<sub>2</sub>). The CO is a common contaminant found in indoor and outdoor environments produced by motorized vehicles, cigarette smoke, and gas stoves. Reducing the use of fossil fuels such as oils and coal has an impact on the reduction of pollution produced by factories and households. The alternative energy that is renewable and considered environmentally friendly can be geothermal, solar or biogas. Each exhaust flue should be equipped with a filter for particulate and gas treatment in order to produce clean air.

Ambient air pollution can be attributed to a variety of adverse health effects. The CO is associated with impaired

neurodevelopmental outcome [4]. The impact of outdoor air pollution exposure for both short and long terms can result in mortality and morbidity of people with COPD [5]. The ambient air pollution with increased concentrations of O<sub>3</sub>, NO<sub>2</sub>, and delicate particulate matter (PM<sub>2.5</sub>) in the short term can be one of the triggers of asthma symptoms [6]. Long-term exposure to soft particulate matter has more influence on mortality from cardiovascular disease than from non-malignant respiratory disease [7]. Therefore, it is necessary to monitor the distribution of air pollution levels regularly in outdoor areas to maintain pollution levels below the air quality guidelines. One way to monitor air pollution is by using a wireless sensor network [8]-[10]. However, this method requires a huge number of sensor nodes for large area coverage. This measurement technique usually has a low spatial resolution. Mobile phones are equipped with gas sensors as portable sensor nodes are used to collect air pollution data with high spatial density in real-time [11]. Mobile robots are used to find gas sources [12]-[14]. However, this method is constrained by several obstacles encountered in the field.

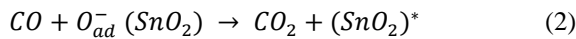
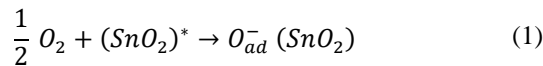
Uncrewed Aerial Vehicle (UAV) is a type of uncrewed aircraft that is useful for monitoring systems in an area. Vertical Take-Off and Landing (VTOL) is one type of UAV that uses many propellers to move. One type of VTOL is a quadcopter that has stability in remote monitoring. The quadcopter can move automatically following the Global

Positioning System (GPS) waypoint guidelines declared by the user [15]-[17]. In this study, we have developed a quadcopter based on the autonomous waypoint navigation used to map the gaseous pollutant of CO in the air.

## II. MATERIALS AND METHOD

### A. Semiconductor Gas Sensor

The gas sensor is a device that measures gaseous pollutants in the air. A metal-oxide-semiconductor is a type of material commonly used as a gas sensor, having a size in the range of 1 - 100 nm, in which this size affects its sensing properties [18]. Fig. 1 shows the structure of the metal oxide semiconductor gas sensor of SnO<sub>2</sub> material. Electrons on the sensor surface inject the atmospheric oxygen around it when the sensor material is heated at a high temperature (~ 400°C). The oxygen ion is adsorbed on the sensor surface, which forms a potential barrier at the grain boundary. This inhibits the flow of electrons and increases the resistance of the sensor material, as shown in Fig. 2(a). When the surface of the material is exposed to reducing gases (e.g., CO), this adsorbed molecule reduces the potential barrier, allowing electrons to flow easily and thereby reduce electrical resistance, as shown in Fig. 2(b). This redox equation can be expressed as:



MQ-7 is a commercial gas sensor to determine the CO concentration represented by an analog voltage, as shown in Fig. 3. The sensitivity characteristic of the sensor is shown in Fig. 4, where R<sub>0</sub> is a sensor resistance at 100 ppm CO in clean air, while R<sub>s</sub> is a sensor resistance at various gas concentrations.

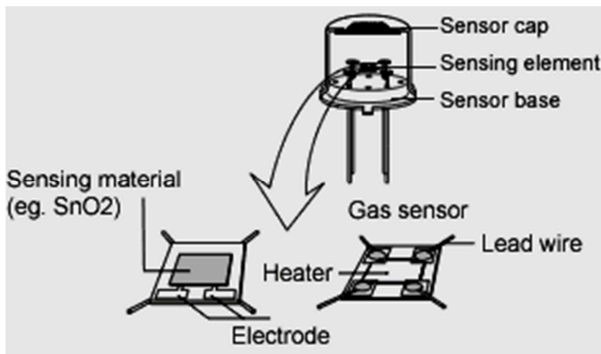


Fig. 1 The metal oxide semiconductor gas sensor.

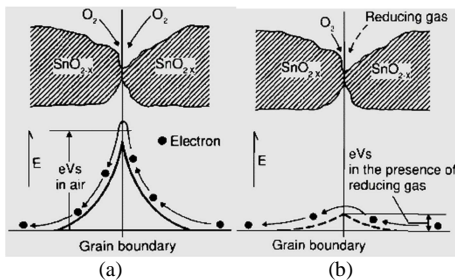


Fig. 2 The inter-grain potential barrier: (a) in the absence of gas, and (b) in the presence of gas [19].

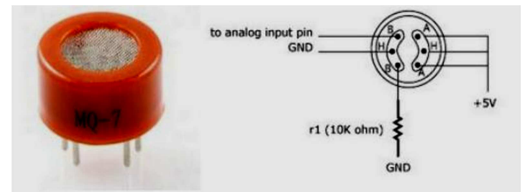


Fig. 3 The MQ-7 gas sensor.

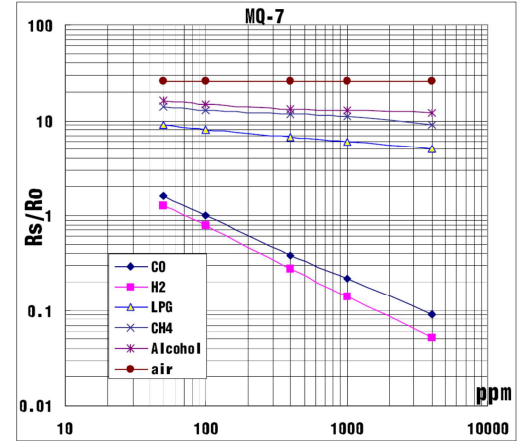
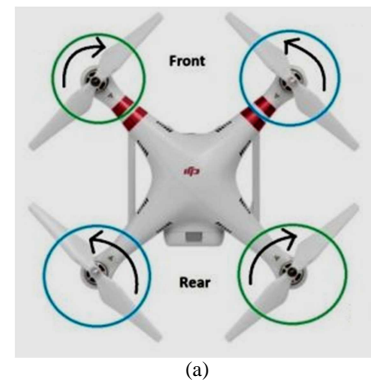


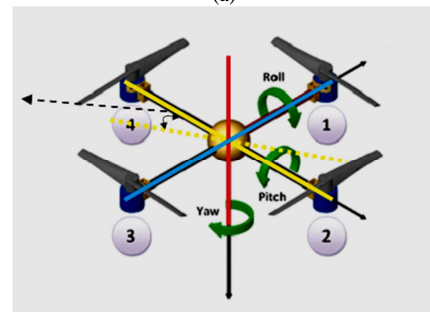
Fig. 4 Sensitivity characteristics of the MQ-7 [20].

### B. Quadcopter System

The quadcopter is the development of a helicopter using synchronization among the four rotors configured in a plus (+) frame. Two pairs of propellers have opposite swivel directions, as shown in Fig. 5 (a). Variations in the speed of the rotors can change the lifting force and direction of the movements, as shown in Fig. 5 (b). The overall block diagram of the electronic system on the quadcopter is shown in Fig. 6. In this study, there are four brushless DC motors installed in the chassis with a size of 55cm x 46cm.



(a)



(b)

Fig. 5 The quadcopter propeller: (a) motor rotation direction, and (b) movement scheme.

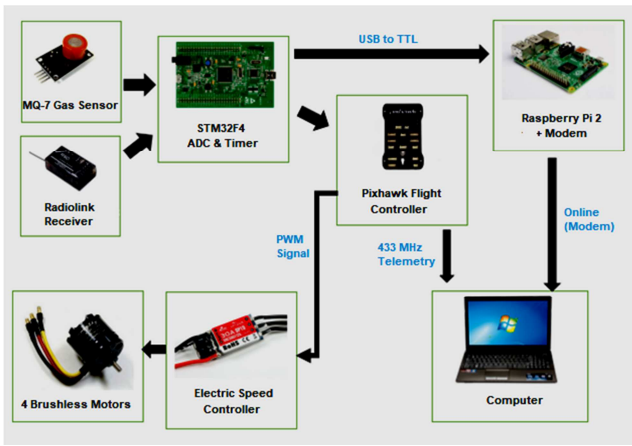


Fig. 6 Block diagram of the quadcopter system.

STM32F4 is a product of ST Electronics that allows users to perform various types of electronic experiments. STM32F407VG is based on 32-bit RISC ARM Cortex-M4, which operates at frequencies up to 168 MHz. The STM32F4 converts the analog signal of the MQ-7 gas sensor into digital data using its internal Analog to Digital Converter (ADC). This processor is equipped with USART for sending and receiving data with other devices.

Raspberry Pi is a single-board computer for teaching in basic computer science. This computer is based on the Broadcom BCM2835 system-on-a-chip, which consists of the ARM1176JZF-S processor with speed ranges from 700 MHz to 1.4 GHz, GPU Video Core IV, and 256 MB RAM. The main operating system on Raspberry Pi uses Debian GNU/Linux and the Python programming language. In this study, Raspberry Pi 2 is used as a data logger and web server of the gas sensor. The 3G modem for online access to web socket is installed on the USB3 port.

Pixhawk is an autopilot system integrated with the processors of STM32F427 Cortex M4 core and is equipped with sensors of gyroscope, accelerometer/magnetometer, accelerometer/gyroscope, and barometer. The Pixhawk module has several pins for different functions, as shown in Fig. 7. This module reads sensor data and drives the four motors to rotate the propellers according to the instructions of the flight controller, as shown in Fig. 8.

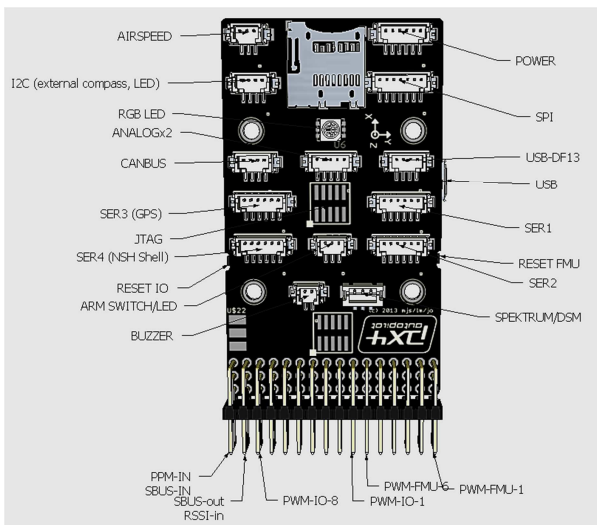


Fig. 7 The configuration of the Pixhawk flight controller.

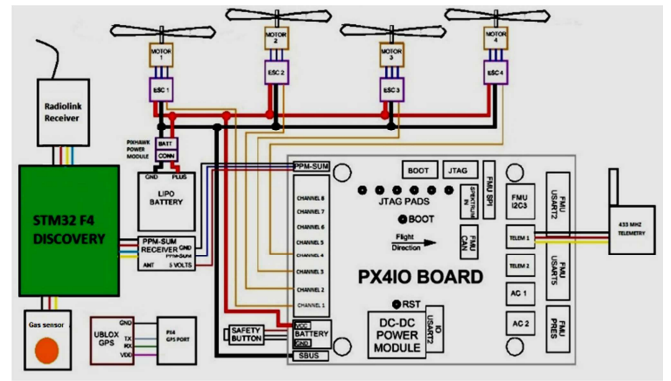


Fig. 8 The Pixhawk controller for the quadcopter system.



Fig. 9 The Mission Planner software is used to provide the waypoints.

The Global Positioning System (GPS) is a satellite-based navigation system that provides location and time information. GPS navigation requires a line of sight of four or more satellites. The U-Blox Neo M8N GPS module has speed, and horizontal position accuracy of 0.05 m/s, and 2.5 m, respectively. The position data from the quadcopter is sent in real-time to the ground station via 433MHz-telemetry.

### C. Navigation of the Quadcopter

The navigation system is an essential part so that the quadcopter can move independently. This study implements a position-based outdoor navigation system using the waypoint method determined by the operator. Therefore, the quadcopter can recognize the position based on the earth coordinate system, correct the direction of motion, and estimate the distances. In this study, mission planner software is used to provide locations or waypoints that must be routed by the quadcopter, as shown in Fig. 9. These waypoints are then entered into the Pixhawk controller via 433 MHz-telemetry.

The proportional-integral-derivative (PID) method is often used to control a mobile robot or UAV movements [21]. The PID equation can be expressed as:

$$u(t) = K_p(t) + K_i \int_0^t e(t')dt' + K_d \frac{de(t)}{dt} \quad (3)$$

where  $K_p$ ,  $K_i$ , and  $K_d$ , are coefficients of the proportional, integral, and derivative, respectively. In this study, the PID control is used to maintain the height of the quadcopter while hovering, as shown in Fig. 10. This is necessary because the position of the quadcopter is often disturbed by environmental factors, mainly the winds.

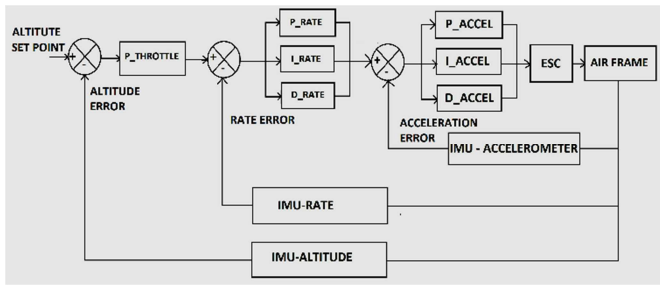


Fig. 10 The altitude control system for the quadcopter.

This control method is applied in the Mission Planner software. For the altitude error, the proportional constant is 4.5 for all the roll, pitch, and *yaw* movements. For rate error, the proportional, integral, and derivative constants are 0.15, 0.1, and 0.004, respectively, for all the roll, pitch, and *yaw* movements. For acceleration error, the values of all the proportional, integral, and derivative constants are 0.15.

### III. RESULTS AND DISCUSSION

The design result of the quadcopter used in this experiment is shown in Fig. 11. The calibration of the MQ-7 gas sensor is carried out with a vehicle exhaust gas sample measured by a commercially available CO meter of AZ-Instrument Model 7701. Fig. 12 shows the gas sensor response to CO concentrations. From the trend line of the sensor response, the gas concentration *X* (ppm) can be predicted by:

$$x = \left( \frac{y}{0.4292} \right)^{3.474635} \quad (4)$$

Where *Y* is the output voltage of the gas sensor (volt), the measurement of CO using the MQ-7 gas sensor has an error of 9.6%, as shown in Table I.

First experiment, the ability to fly of the quadcopter is tested in area of 30m x 12m, as shown in Fig. 13. Table II shows the waypoints routed by the quadcopter with the altitude setpoint of 4 meters. These waypoints are displayed on Google Maps, as shown in Fig. 14. In loiter mode, the quadcopter automatically attempts to maintain the current position. At a certain position near waypoint 2, there is a gas produced by combustion.



Fig. 11 The quadcopter used in the experiment.

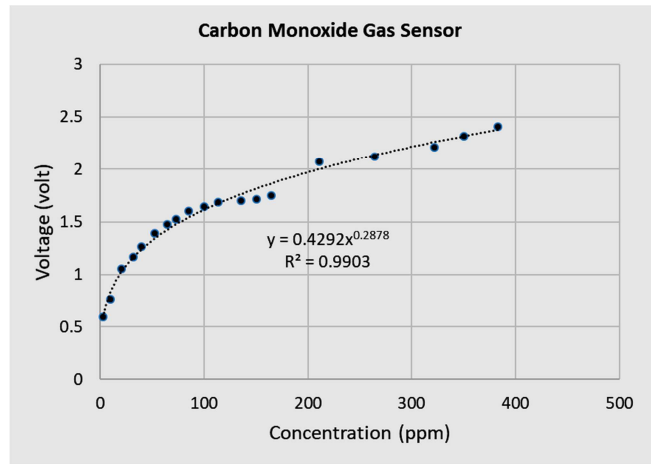


Fig. 12 The MQ-7 gas sensor response to CO concentration.

TABLE I  
COMPARISON OF THE MQ-7 GAS SENSOR AND THE CO METER.

CO-meter (ppm)	Gas Sensor (ppm)	Error (%)
3	3.02	0.70
10	7.62	23.79
21	22.98	9.45
32	32.61	1.89
40	43.12	7.79
53	59.48	12.22
65	73.09	12.45
73	81.69	11.90
85	97.58	14.80
100	106.31	6.30
114	117.00	2.63
136	120.16	11.64
151	123.62	18.12
165	131.56	20.27
211	237.92	12.76
264	257.20	2.57
322	297.17	7.71
350	351.81	0.52
383	401.55	4.84
<b>Average Error</b>		<b>9.6</b>



Fig. 13 The location of testing the quadcopter for flying.

The experimental results show that the quadcopter can follow all the provided waypoints, which are accompanied by information about the CO gas concentration displayed on Google Earth, as shown in Fig. 15. Meanwhile, Gb. 16 shows a detailed graph of the gas level against the time displayed on the Plotly web server.

TABLE II  
THE GPS WAYPOINTS USED FOR QUADCOPTER NAVIGATION WITH A 4-METER ALTITUDE SETPOINT.

No	Mission	Altitude (meters)	Latitude	Longitude
1	Waypoint 1	4	-7.2843360	112.797474
2	Loiter (WP 2)	4	-7.2844315	112.797518
3	Waypoint 3	4	-7.2845432	112.797529
4	Waypoint 4	4	-7.2845512	112.797365
5	Waypoint 5	4	-7.2844554	112.797341
6	Loiter (WP 6)	4	-7.2843570	112.797410

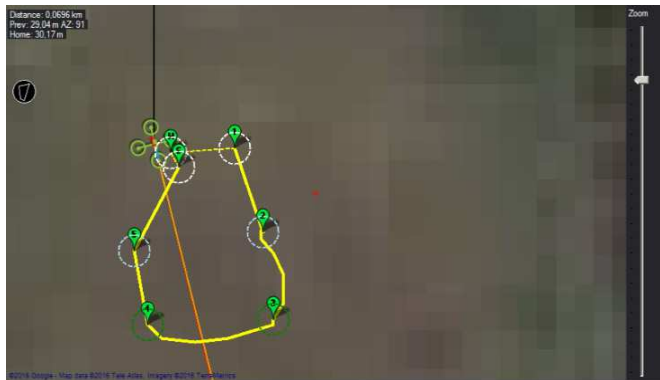


Fig. 14 Declaration of the waypoints on Google Maps in the Mission Planner software.



Fig. 15 The result of gas mapping carried out by the quadcopter.

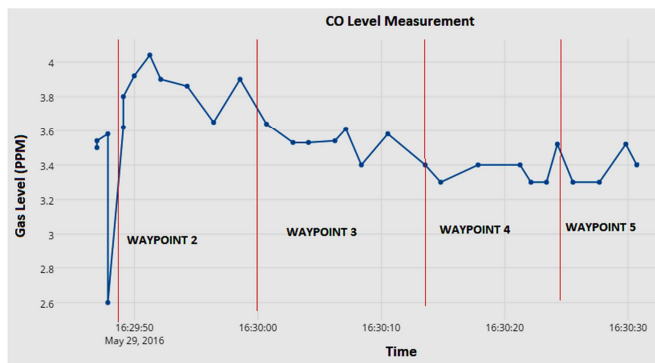


Fig. 16 The result of gas levels displayed on the Plotly web server.

Fig. 17 shows the barometer altitudes starting from take-off to landing of the quadcopter. This quadcopter tries to maintain the height according to the provided altitude setpoint. The result of this altitude control has a steady-state error of about 15.75%, as shown in Table III.

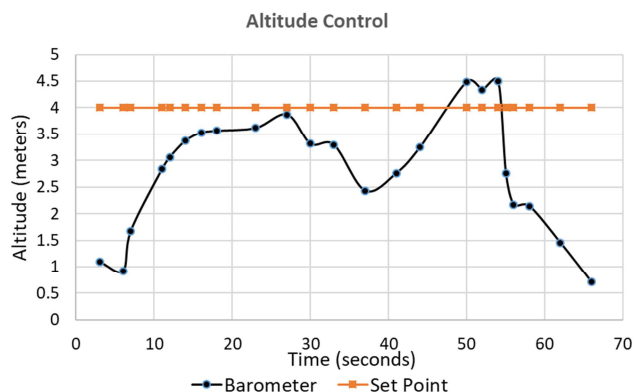


Fig. 17 The result of altitude control starting from take-off to landing of the quadcopter for a 4-meter setpoint.

TABLE III  
THE RESULT OF ALTITUDE CONTROL ON THE QUADCOPTER FOR A 4-METER ALTITUDE SETPOINT.

Set Point (meters)	Barometer Altitude (meters)	Error (%)
4	3.372125	15.69
4	3.525146	11.87
4	3.561984	10.95
4	3.615825	9.60
4	3.870860	3.22
4	2.431133	39.22
4	2.762876	30.92
4	4.491366	12.28
4	4.341257	8.53
4	2.760042	30.99
<b>Average Error</b>		<b>15.75</b>

TABLE IV  
THE GPS WAYPOINTS USED FOR QUADCOPTER NAVIGATION WITH A 3-METER ALTITUDE SETPOINT.

No	Mission	Altitude (meters)	Latitude	Longitude
1	Waypoint 1	3	-7.2843157	112.797487
2	Loiter (WP 2)	3	-7.2844088	112.797493
3	Loiter (WP 3)	3	-7.2844793	112.797459
4	Waypoint 4	3	-7.2845312	112.797399
5	Loiter (WP 5)	3	-7.2844550	112.797342
6	Loiter (WP 6)	3	-7.2843157	112.797408



Fig. 18 The waypoints on Google Maps in the Mission Planner software.

In the second experiment, the ability to fly the quadcopter is tested with the altitude setpoint of 3 meters. Table IV and Fig. 18 show the waypoints that will be routed by the quadcopter. There is a CO gas source laid near the waypoint 2 as well. The quadcopter can follow the waypoints, as shown in Fig. 19, and the detailed graph of the gas level is shown in Fig. 20. Fig. 21 shows that this quadcopter never reaches the provided altitude setpoint with the steady-state error of about 21.4%, as shown in Table V.



Fig. 19 The gas mapping carried out by the quadcopter.

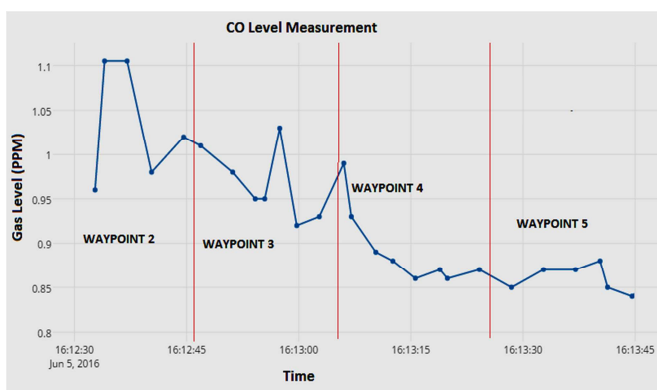


Fig. 20 The gas levels displayed on the Plotly web server.

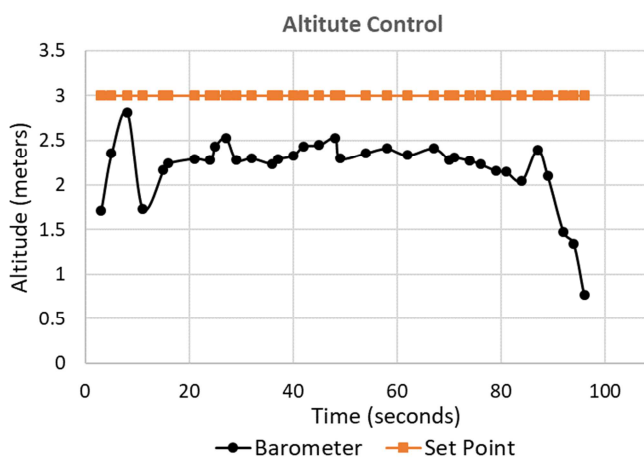


Fig. 21 The altitude control for a 3-meter setpoint.

TABLE V  
THE RESULT OF ALTITUDE CONTROL ON THE QUADCOPTER FOR A 3-METER ALTITUDE SETPOINT.

Set Point (meters)	Barometer Altitude (meter)	Error (%)
3	2.16679	27.77
3	2.242084	25.26
3	2.434502	18.84
3	2.529316	15.68
3	2.233718	25.54
3	2.28914	23.69
3	2.331321	22.28
3	2.529316	15.68
3	2.409404	19.68
3	2.412192	19.59
<b>Average Error</b>		<b>21.4</b>

#### IV. CONCLUSIONS

In this study, we have developed UAV to map the gaseous pollutant based on autonomous waypoint navigation. The system consists of quadcopter equipped with metal oxide semiconductor type CO gas sensor, Pixhawk controller, GPS, radio telemetry, STM32F4 and Raspberry Pi 2 microcomputers. Mission Planner software is used to provide locations or waypoints. The PID control is used to maintain the altitude of the quadcopter while hovering. The information about the CO gas distributions is displayed on Google Earth. The experiment results show that the measurement of CO using the MQ-7 gas sensor has an error of 9.6%. The quadcopter can route all the provided waypoints for its navigation. The quadcopter can also maintain the height according to the provided altitude setpoints of 3 and 4 meters with a steady-state error about 21.4 % and 15.75%, respectively.

#### ACKNOWLEDGMENT

This research was carried out with financial aid support from Lembaga Penelitian dan Pengabdian Kepada Masyarakat (LPPM) Institut Teknologi Sepuluh Nopember (ITS) Surabaya, and the Ministry of Research, Technology and Higher Education of the Republic of Indonesia (Kemenristekdikti RI).

#### REFERENCES

- [1] B.P. Resosudarmo and L. Napitupulu, "Health and Economic Impact of Air Pollution in Jakarta," *The Economic Record*, 80, pp. S65-S75, 2004.
- [2] B. Dobbie and D. Green, "Australians are not equally protected from industrial air pollution," *Environ. Res. Lett.*, 10, pp. 1-13, 2015.
- [3] W. Du, X. Li, Y. Chen, and G. Shen, "Household air pollution and personal exposure to air pollutants in rural China - A review," *Environmental Pollution*, 237, pp. 625-638, 2018.
- [4] R.J. Levy, "Carbon monoxide pollution and neurodevelopment: A public health concern," *Neurotoxicology and Teratology*, 49, pp. 31-40, 2015.
- [5] Y. Liu, S. Yan, K. Poh, S. Liu., E. Lyrioriobhe, and D.A. Sterling, "Impact of air quality guidelines on COPD sufferers", *International Journal of COPD*, 11, pp. 839-872, 2016.
- [6] J.K. Wendt, E. Symanski, T.H. Stock, W. Chan, and X.L. Du, "Association of short-term increases in ambient air pollution and timing of initial asthma diagnosis among medicaid-enrolled children in a metropolitan area," *Environ Res.*, 131, pp. 50-58, May 2014.
- [7] G. Hoek, R.M. Krishnan, R. Beelen, A. Peters, B. Ostro, B. Brunekreef and J.D. Kaufman, "Long-term air pollution exposure and cardio-respiratory mortality: a review," *Environmental Health*, 12:43, pp. 1-16, 2013.

- [8] C. Peng, K. Qian, and C. Wang, "Design and Application of a VOC-Monitoring System Based on a ZigBee Wireless Sensor Network," *IEEE Sensors Journal*, Vol. 15, No. 4, pp. 2255-2268, April 2015.
- [9] L. Bao, and H. Wang, "Distributed real-time monitoring system for atmospheric particles," *IET Wireless Sensor Systems*, Vol. 7 Iss. 4, pp. 91-97, 2017.
- [10] H. Yang, Y. Qin, G. Feng, and H. Ci, "Online Monitoring of Geological CO<sub>2</sub> Storage and Leakage Based on Wireless Sensor Networks", *IEEE Sensors Journal*, Vol. 13, No. 2, pp. 556-562, Feb. 2013.
- [11] K. Hu, V. Sivaraman, B.G. Luxan, and A. Rahman, "Design and Evaluation of a Metropolitan Air Pollution Sensing System", *IEEE Sensors Journal*, Vol. 16, No. 5, pp. 1448-1459, March 2016.
- [12] M. Rivai, Rendyansyah, D. Purwanto, "Implementation of Fuzzy Logic Control in Robot Arm for Searching Location of Gas Leak," in *International Seminar on Intelligent Technology and Its Application*, 2015, pp. 69-74.
- [13] A.S.A. Yeon, R. Visvanathan, S.M. Mamduh, K. Kamarudin, L.M. Kamarudin, and A. Zakaria, "Implementation of behaviour based robot with sense of smell and sight," *Procedia Computer Science*, 76, 2015, pp. 119-125.
- [14] R. Watiasih, M. Rivai, R.A. Wibowo, O. Penangsang, "Path Planning Mobile Robot Using Waypoint for Gas Level Mapping", in *International Seminar on Intelligent Technology and Its Application*, 2017, pp. 244-249.
- [15] E. Yanmaz, S. Yahyanejad, B. Rinner, H. Hellwagner, and C. Bettstetter, "Drone networks: Communications, coordination, and sensing," *Ad Hoc Networks*, 68, pp. 1-15, 2018.
- [16] G.J. Fouché, and R. Malekian, "Drone as an autonomous aerial sensor system for motion planning," *Measurement*, 119, pp. 142-155, 2018.
- [17] A. Clark, "Small unmanned aerial systems comparative analysis for the application to coastal erosion monitoring," *GeoResJ*, 13, pp. 175-185, 2017.
- [18] A. Dey, "Semiconductor metal oxide gas sensors: A review," *Materials Science & Engineering*, B 229, pp. 206-217, 2018.
- [19] "General Information for TGS Sensors data sheet," Figaro USA Inc., Glenview, IL 60026 USA
- [20] "Technical Data MQ-7 Gas Sensor data sheet," Hanwei Electronics Co., LTD.
- [21] T.T. Mac, C. Copot, R.D. Keyser, and C.M. Ionescu, "The development of an autonomous navigation system with optimal control of an UAV in partly unknown indoor environment," *Mechatronics*, 49, pp. 187-196, 2018.